DNA methylation and histone H1 cooperatively repress transposable elements and aberrant intragenic transcripts

Jaemyung Choi[1], David B. Lyons[2], M. Yvonne Kim[2], Jonathan D. Moore[1] and Daniel Zilberman[1,*]

[1]Department of Cell & Developmental Biology, John Innes Centre, Norwich, NR4 7UH, UK

[2]Department of Plant & Microbial Biology, University of California, Berkeley, CA 94720, USA

*Correspondence: daniel.zilberman@jic.ac.uk

Summary

DNA methylation and histone H1 mediate transcriptional silencing of genes and transposable elements, but how they interact is unclear. In plants and animals with mosaic genomic methylation, functionally mysterious methylation is also common within constitutively active housekeeping genes. Here we show that H1 is enriched in methylated sequences, including genes, of *Arabidopsis thaliana*, yet this enrichment is independent of DNA methylation. Loss of H1 disperses heterochromatin, globally alters nucleosome organization, and activates H1-bound genes, but only weakly de-represses transposable elements. However, H1 loss strongly activates transposable elements hypomethylated through mutation of DNA methyltransferase *MET1*. Loss of H1 also activates antisense transcripts within demethylated genes. Our results demonstrate that H1 and DNA methylation cooperatively maintain transcriptional homeostasis by silencing transposable elements and aberrant intragenic transcripts. Such functionality plausibly explains why DNA methylation, a well-known mutagen, has been maintained within coding sequences of crucial plant and animal genes.

Keywords: DNA methylation, gene body methylation, histone H1, transcriptional silencing, antisense transcription.

Highlights

- Histone H1 is enriched in methylated DNA independently of methylation
- Loss of H1 activates genes, alters nucleosome organization and disperses heterochromatin
- DNA methylation and H1 jointly silence transposons
- DNA methylation and H1 cooperatively suppress intragenic antisense transcripts

22 **Introduction**

23 Cytosine DNA methylation is an epigenetic modification that protects genome integrity by
24 repressing transposable elements (TEs) in plants, vertebrates, fungi, and likely other eukaryotic
25 groups (Du et al., 2015; Jones, 2012; Zemach and Zilberman, 2010). Methylation of regulatory
26 sequences, such as promoters and enhancers, also causes gene silencing in plants and vertebrates
27 (Hon et al., 2013; Jones, 2012; Schübeler, 2015; Zhang et al., 2018a). Proper patterns of DNA
28 methylation are essential for plant and animal development (Iurlaro et al., 2017; Kawashima and
29 Berger, 2014; Schmidt et al., 2015; Smith and Meissner, 2013), and their disruption is linked with
30 cancer and other serious diseases (Jones et al., 2016; Rasmussen and Helin, 2016; Robertson,
31 2005).

32 Despite its association with transcriptional repression, DNA methylation is common within
33 active genes (Bewick and Schmitz, 2017; Feng et al., 2010; Jones, 2012; Zemach et al., 2010).
34 Vertebrate intragenic methylation occurs in the context of a globally methylated genome, in which
35 methylation is the default state and some sequences, including active promoters and enhancers, are
36 protected from methylation (Schübeler, 2015; Suzuki and Bird, 2008). Mammalian genes are co-
37 transcriptionally hypermethylated by the *de novo* methyltransferase Dnmt3 (Baubec et al., 2015;
38 Morselli et al., 2015; Neri et al., 2017), and – likely due to this activity – mammalian intragenic
39 methylation is positively correlated with gene expression (Lister et al., 2009; Yang et al., 2014).
40 Several functions have been ascribed to mammalian intragenic methylation, including the
41 silencing of intragenic promoters and enhancers (Deaton et al., 2011; Hellman and Chess, 2007;
42 Kulis et al., 2012; Maunakea et al., 2010; Yang et al., 2014), regulation of splicing (Lev Maor et
43 al., 2015; Maunakea et al., 2013; Shukla et al., 2011), and suppression of aberrant transcripts (Neri
44 et al., 2017). However, the latter function has been questioned, because strong DNA methylation

45 loss in mouse embryonic stem cells was not associated with activation of intragenic transcription
46 (Teissandier and Bourc'his, 2017).

47 In contrast to vertebrates, plant and invertebrate genomes usually have mosaic methylation
48 patterns, with specific sequences targeted for methylation (Schübeler, 2015; Suzuki and Bird,
49 2008). In flowering plants, TEs and gene bodies are preferentially methylated (Bewick and
50 Schmitz, 2017; Lister et al., 2008; Takuno and Gaut, 2013; Zemach and Zilberman, 2010). TEs
51 are affected by multiple pathways that mediate methylation in three sequence contexts (CG, CHG
52 and CHH, where H ≠ G), whereas only CG sites are methylated in genes (Feng et al., 2010; Zemach
53 et al., 2010; Zhang et al., 2018a). Invertebrates preferentially or exclusively methylate gene bodies,
54 and essentially all methylation is in the CG context (Bewick et al., 2017; Dixon et al., 2016; Feng
55 et al., 2010; Suzuki et al., 2007; Zemach et al., 2010). Plant and invertebrate intragenic methylation
56 is not directly linked to transcription, but is instead a largely invariant genomic feature that
57 decorates the same sets of genes across developmental stages and tissues (Bartels et al., 2018;
58 Libbrecht et al., 2016; Suzuki et al., 2013; Zemach et al., 2018). This phenomenon, commonly
59 called gene body methylation (gbM), is concentrated in the exons of evolutionarily conserved,
60 stably and constitutively expressed genes, and is maintained by the methyltransferase Dnmt1
61 (called MET1 in plants) (Bewick and Schmitz, 2017; Bewick et al., 2018; Cokus et al., 2008;
62 Dixon et al., 2016; Lister et al., 2008; Sarda et al., 2012; Takuno and Gaut, 2012, 2013; Zemach
63 and Zilberman, 2010). GbM has been proposed to regulate splicing and transcriptional elongation,
64 and to suppress intragenic transcriptional initiation (Hunt et al., 2013; Regulski et al., 2013; Suzuki
65 et al., 2007; To et al., 2015; Tran et al., 2005; Zilberman et al., 2007). However, loss of gbM in
66 the flowering plant *Arabidopsis thaliana* and the insect *Oncopeltus fasciatus* is not associated with
67 transcriptional changes (Bewick et al., 2016, 2018; Kawakatsu et al., 2016), and gbM is commonly

68 thought to be a nonfunctional byproduct of TE methylation (Bewick and Schmitz, 2017; Bewick
69 et al., 2016; Teixeira and Colot, 2009). Overall, the functions of gbM – if any exist – remain
70 mysterious (Zhang et al., 2018a; Zilberman, 2017).

71 A potential explanation for the mystery and controversy surrounding gbM – and intragenic
72 methylation in general – is that its function is subtle and shared with other chromatin factors. This
73 hypothesis was tested in the flowering plant *Arabidopsis thaliana* by simultaneously eliminating
74 gbM and trimethylation of lysine 36 of histone H3, a histone modification that suppresses cryptic
75 intragenic transcripts and regulates splicing (Carrozza et al., 2005; Wagner and Carpenter, 2012),
76 but no transcriptional or RNA processing defects attributable to gbM were found (Bewick et al.,
77 2016). A plausible alternate candidate is histone H1, a protein that binds nucleosomes and the
78 intervening linker DNA (Fyodorov et al., 2018; Hergeth and Schneider, 2015; Over and Michaels,
79 2014). Like methylation, H1 is associated with transcriptional silencing but is nevertheless
80 abundant in active plant and animal genes (Krishnakumar et al., 2008; Rutowicz et al., 2015;
81 Torres et al., 2016). There is also evidence that H1 preferentially inhibits transcriptional initiation
82 from methylated DNA *in vitro* (Johnson et al., 1995; Levine et al., 1993). These data suggest that
83 H1 and DNA methylation may act cooperatively, including within gene bodies. However, whether
84 H1 affinity is regulated by DNA methylation is uncertain, with some studies finding preferential
85 association with methylated DNA (Levine et al., 1993; McArthur and Thomas, 1996), and others
86 reporting no preference (Campoy et al., 1995; Hashimshony et al., 2003; Nightingale and Wolffe,
87 1995). More generally, if and how H1 interacts with methylation *in vivo* to regulate transcription
88 is unknown.

89 **Results**

90 **Histone H1 is enriched in methylated DNA independently of methylation**

91 To investigate the functional relationship between DNA methylation and H1, we analyzed the
92 genomic distribution of the two major *Arabidopsis* H1 proteins, H1.1 and H1.2 (Over and
93 Michaels, 2014). Consistent with earlier work (Rutowicz et al., 2015), we did not find any salient
94 differences between H1.1 and H1.2 (Figure S1A), and therefore will refer simply to H1. As
95 expected, H1 preferentially associates with linker DNA (Figures 1A and S1B), is concentrated in
96 heavily methylated heterochromatic TEs (Figures 1B, 1C, S1C and Table S1), and is abundant
97 within genes, particularly those with low/no expression (Figures 1D and S1D). H1 is also enriched
98 in methylated genes compared to similarly expressed unmethylated genes (Figures 1E and S1E).
99 Thus, H1 is preferentially associated with methylated DNA in *Arabidopsis.*

100 To determine if DNA methylation affects H1 binding, we analyzed H1 distribution in *met1*
101 mutant plants. The *met1* mutation eliminates CG methylation, which includes the entirety of gbM
102 (Cokus et al., 2008; Lister et al., 2008). Many TEs also lose non-CG methylation and dimethylation
103 of lysine 9 of histone H3 (H3K9me2), a mark of heterochromatin (Feng and Michaels, 2015), and
104 become more accessible to DNase I (MET1-dependent TEs, Figure 1F) (Deleris et al., 2012; Zhang
105 et al., 2018b). We find that H1 distribution is well-correlated between wild type (*wt*) and *met1*
106 (Figures 1B, 1C, 1F, 1G and S1C, S1F). Genes methylated in *wt* retain higher levels of H1 in *met1*
107 plants (Figures 1E and S1E), as do TEs (Figures 1C and S1C). Therefore, H1 binding is largely
108 independent of DNA methylation. However, some TEs do lose H1 in *met1* mutants, particularly
109 MET1-dependent TEs that are transcriptionally activated (Figures 1F and S1G).

110 To determine how H1 distribution is regulated, we analyzed H1 association with various
111 genomic features using principal component analysis. H1 associates most strongly with GC

112 content (Figure 1H) independently of nucleosome density (Figure S1H). Methylated genes have
113 elevated GC content (Figure S1I), which likely explains their H1 enrichment (Figures 1E and S1E).
114 H1 also associates with heterochromatic features, including DNA methylation and H3K9me2,
115 along the first principal component (Figure 1H), and is well-separated from features of active
116 transcription (such as H3K4me3, Figure 1H). Based on these results, we used GC content and *wt*
117 H3K9me2 and H3K4me3 data to create a linear regression model of H1 abundance. This model
118 accurately describes *wt* H1 distribution across genes and TEs (Figures 1B, 1F, 1I, 1J, and S1J-L),
119 including H1 enrichment in methylated genes (Figures 1E and S1K). More importantly, our model
120 successfully predicts *met1* H1 distribution (Figures 1B, 1E, 1F, 1J and S1J-L), including the loss
121 of H1 from a subset of MET1-dependent (*i.e.* heterochromatin-deficient) TEs (Figures 1F and
122 S1G). Thus, H1 enrichment can largely be explained by sequence composition, transcription, and
123 heterochromatin, whereas DNA methylation has little, if any direct effect on H1 binding.
124
125 **Histone H1 mediates global nucleosome organization**
126 The distribution of *Arabidopsis* H1 (heterochromatin > silent genes > active genes, Figures 1B-D)
127 corresponds to an unexplained phenomenon in the human genome, in which genes expressed at
128 higher levels have shorter average nucleosome repeat length (NRL) than less expressed genes,
129 which have shorter average NRLs than heterochromatin (Valouev et al., 2011). Because loss of
130 H1 is known to reduce the average NRL in animal genomes (Baldi et al., 2018; Fan et al., 2003;
131 Woodcock et al., 2006), we tested the hypothesis that H1 causes the observed NRL differences by
132 comparing nucleosome spacing between plants with defective *H1.1* and *H1.2* genes (*h1* mutants)
133 (Zemach et al., 2013) and *wt* controls.

134 As in the human genome, *Arabidopsis* genes expressed at higher levels have shorter
135 average NRL in *wt* (Figure 2A). The NRL of less-expressed, H1-rich genes decreases substantially
136 in *h1* mutants (Figures 2A-C and S2A). In the most H1-rich genes, mean NRL is reduced from
137 185 bp to 169 bp (Figures 2B and 2C), which is consistent with the ability of H1 to protect about
138 20 bp of DNA *in vitro* (Simpson, 1978). Consistent with published results (Zhang et al., 2015), we
139 find that heterochromatic TEs have longer average NRLs than more euchromatic TEs (Figure 2D),
140 with the longest NRLs in the most H1-rich TEs (Figure 2E). Loss of H1 reduces mean NRL of
141 H1-rich TEs by 22 bp (from 189 bp to 167 bp), causing TEs in *h1* mutants to have similar NRLs
142 regardless of their *wt* H1 levels (Figures 2E, 2F and S2B). The average NRLs of TEs and silent
143 genes are also very similar in *h1* plants (Figure S2C). Thus, H1 is an important global regulator of
144 nucleosome placement that accounts for much of the average NRL difference across the
145 *Arabidopsis* genome.
146
147 **Loss of H1 activates transcription and disperses heterochromatin**
148 Histone H1 mediates gene silencing (Fyodorov et al., 2018; Krishnakumar et al., 2008; Torres et
149 al., 2016) and the 3D configuration of heterochromatin (Cao et al., 2013; Lu et al., 2009) in
150 animals, but the effects of H1 on transcription and higher order chromatin organization in plants
151 are unknown. To understand how H1 regulates transcription, we determined mRNA levels using
152 RNA-seq in *h1* mutants in comparison to *wt*. Most of the significantly mis-regulated genes in
153 leaves and seedlings (707/990, 71%) are upregulated in *h1* plants (Figures 3A, 3B and Table S2).
154 These genes are H1-enriched (Figures 3C, 3D and S3A) and are transcribed at low levels in *wt*
155 (Figure 3E), indicating that H1 can repress gene transcription in plants. However, given that H1 is
156 generally abundant in *Arabidopsis* genes (Figures 1C and 1D), its effects on transcription are fairly

157 selective, as is the case in animals (Fan et al., 2005). Several gene ontology functional categories
158 are overrepresented among the upregulated genes, most notably categories related to the meiotic
159 cell cycle and meiotic recombination (Figure S3B and Table S2). Upregulated genes include
160 ASYNAPTIC (ASY) 1 and 4, and other key meiotic genes (Figures 3B, 3F and Table S2)
161 (Chambon et al., 2018; Mercier et al., 2015). H1 is depleted in male and female *Arabidopsis*
162 meiocytes (She and Baroux, 2015; She et al., 2013), suggesting H1 removal may help to activate
163 the meiotic transcriptional program. Genes involved in epigenetic silencing are also preferentially
164 upregulated (Figure S3B and Table S2). Curiously, one of these is ARGONAUTE9 (Figure 3B),
165 which is involved in meiocyte specification (Olmedo-Monfil et al., 2010), further reinforcing the
166 link between H1 and meiocyte fate and function.

167 In *wt Arabidopsis*, heterochromatin is arranged into large DAPI-stained foci called
168 chromocenters (Figures 4A and S4A) (Ascenzi and Gantt, 1999; Fransz et al., 2002). We find that
169 in *h1* mutants nuclei typically have few chromocenters and many smaller DAPI-stained foci
170 (Figures 4A, 4B and S4A), indicating that the role of H1 in heterochromatin organization is
171 generally conserved. However, despite the dispersal of chromocenters, only 32 TEs are
172 significantly upregulated in *h1* plants (Table S2). An important consideration is that H1 is a major
173 regulator of *Arabidopsis* DNA methylation: depletion of H1 increases methylation of some TEs in
174 all sequence contexts, and reduces methylation of other TEs (Lyons and Zilberman, 2017;
175 Rutowicz et al., 2015; Wierzbicki and Jerzmanowski, 2005; Zemach et al., 2013). Most of the
176 upregulated TEs (29, 91%) are hypomethylated in *h1* mutants (Figures 4C-E and S4B), suggesting
177 that some of the observed activation is not directly caused by H1 depletion. Furthermore,
178 heterochromatin does not become substantially more accessible to DNase I in *h1* mutants (Figure

179 4F). Thus, although heterochromatin is altered (Figures 2D-F) and dispersed (Figures 4A, 4B and
180 S4A) by lack of H1, heterochromatic functionality remains largely intact.
181
182 **DNA methylation and H1 cooperatively silence TEs**
183 Limited TE activation in *h1* plants contrasts with the extensive TE upregulation in H1-deficient
184 *Drosophila melanogaster* (Iwasaki et al., 2016; Lu et al., 2013), but is similar to the effects of H1
185 depletion on mouse cells, which show few changes in TE expression (Fan et al., 2005). TEs are
186 silenced by DNA methylation in mouse and *Arabidopsis* (Law and Jacobsen, 2010), whereas
187 *Drosophila* lacks cytosine methylation (Raddatz et al., 2013; Zemach et al., 2010), suggesting that
188 the effects of H1 loss may be masked by methylation. To test this hypothesis, we investigated TE
189 expression in *h1met1* compound mutants and *met1* controls.
190 Because H1 can locally raise or lower DNA methylation (Rutowicz et al., 2015; Zemach
191 et al., 2013), we first identified active TEs with unchanged CHG and CHH methylation near the
192 transcriptional start site (TSS) between *met1* and *h1met1*, which turned out to be mostly TEs that
193 are fully demethylated in both genotypes (Figures 5A, 5B, S5A and Table S3). Unsupervised
194 clustering separated these TEs into two groups, both of which become much more accessible to
195 DNase I in *met1* and remain so in *h1met1* (Figures 5A and S5B). The larger group (nc; 272 TEs)
196 is expressed similarly in *met1* and *h1met1* (Figure 5A). However, the smaller group of TEs (up1;
197 134) is strongly upregulated in *h1met1* (Figures 5A and S5C). These TEs are significantly H1-
198 enriched in *met1* compared to TEs with unchanged expression, especially around the TSS (Figures
199 5C, 5D and S5D). These TEs are thus apparently transcriptionally repressed by H1 and DNA
200 methylation. Loss of methylation alone leads to mild activation and locus accessibility, but loss of
201 both methylation and H1 is required to create a highly active state (Figures 5A and S5B).

202 Analysis of TEs with altered TSS-proximal CHG or CHH methylation produced three
203 groups, all of which maintain robust non-CG methylation in *met1* and *h1met1* (Figure 5E and Table
204 S3). All three groups are more accessible to DNase I in *h1met1* compared to *met1* (Figures 5E and
205 S5B), indicating that loss of H1 increases the accessibility of partially demethylated sequences.
206 The first group (up2) is comprised of 63 TEs upregulated and hypomethylated in *h1met1* compared
207 to *met1* (Figures 5E and S5E). The second group (dn) consists of 147 TEs downregulated and
208 hypermethylated in *h1met1* (Figures 5E and S5F). Thus, both groups are likely differentially
209 expressed between *met1* and *h1met1* due to changes in DNA methylation. However, the third –
210 and largest – group (up3; 159 TEs) is upregulated in *h1met1* despite substantial hypermethylation
211 (Figures 5E, 5F and S5G). Compared to the dn group, these TEs are significantly H1-enriched
212 (Figures 5G, 5H and S5D). TEs in the up3 group, like those in group up1 described above, are
213 mildly activated in *met1* and require loss of H1 for strong expression (Figure 5E). These data
214 indicate that DNA methylation and H1 jointly create an inaccessible chromatin state that silences
215 TEs.
216
217 **DNA methylation and H1 cooperatively suppress intragenic antisense transcripts**
218 The ability of H1 and DNA methylation to cooperatively repress transcription, and enrichment of
219 H1 within methylated genes (Figure 1E), are consistent with the possibility that methylation and
220 H1 act together to reduce aberrant intragenic transcripts, a long-hypothesized function of gbM
221 (Tran et al., 2005; Zilberman et al., 2007). To test this hypothesis, we identified antisense
222 intragenic transcripts with significantly altered expression in *h1, met1* and *h1met1* mutants in
223 comparison to *wt*. We identified 17 such transcripts in *h1*, most of which (15, 88%) are upregulated
224 (Figure 6A). This result is consistent with the hypothesis that H1 suppresses intragenic

225 transcription, but the small number of identified transcripts limits confidence and prevents further
226 analysis. We found many more mis-expressed antisense transcripts in *met1* (468), and yet more in
227 *h1met1* (1152; Figure 6A). In *met1,* only 32% of transcripts (149) are upregulated (Figure 6A). In
228 contrast, 91% of transcripts (1044) are upregulated in *h1met1* (Figure 6A), supporting the
229 hypothesis that intragenic transcription is de-repressed when DNA methylation and H1 are
230 simultaneously absent.

231 We next separated antisense transcripts for which the change in expression is positively
232 correlated with the sense transcript from those with an absent or negative correlation (some
233 antisense transcripts were ambiguously correlated and therefore were removed from this analysis).
234 A positive correlation suggests that antisense expression is altered due to increased or decreased
235 overall transcriptional activity at the locus, whereas uncorrelated or negatively correlated antisense
236 transcription must be regulated differently. In *met1* plants, sense and antisense expression is
237 correlated in most cases (65%, 262 out of 403 transcripts in Figure 6B and Table S4), indicating
238 that the antisense transcriptional changes we detected are mainly due to mis-regulation of sense
239 transcripts. However, negatively or un-correlated, upregulated antisense transcripts are much more
240 likely to initiate from methylated DNA than positively correlated, downregulated, or unchanged
241 transcripts (Figures 6B and 6C). This result suggests that antisense expression is activated by
242 methylation loss, but we identified just 47 (12%) such transcripts (Figures 6B and 6C). Thus, *met1*
243 data provide only modest support for the hypothesis that gbM suppresses antisense expression.

244 The situation is substantially different in *h1met1* plants, in which antisense expression is
245 most commonly upregulated and not positively correlated with sense expression (83%, 894 out of
246 1074 transcripts in Figure 6D and Table S4). As in *met1,* these transcripts are much more likely to

247 initiate from DNA methylated in *wt* than other antisense transcripts (Figures 6D-F and S6A, S6B),
248 indicating that gbM and H1 cooperatively silence antisense transcription.

249 To further analyze the link between gbM and antisense expression, we separated all the
250 antisense transcripts we annotated (regardless of their behavior in mutant genotypes) into three
251 groups based on their point of initiation: those from methylated DNA, from unmethylated DNA
252 within methylated genes, or from unmethylated genes (Figure 6G). As expected, transcripts that
253 initiate from methylated DNA have more H1 around the TSS (Figures 6H and S6C, S6D). In *met1*,
254 levels of transcripts arising from methylated genes are significantly elevated compared to
255 unmethylated genes (Figure 6I). Transcripts initiating from methylated sequences are also
256 significantly elevated compared to those initiating from unmethylated regions of methylated genes
257 (Figure 6I). In *h1met1*, levels of transcripts arising from methylated genes are also significantly
258 elevated, and transcripts initiating from methylated DNA are especially upregulated (Figure 6I),
259 specifically linking methylation loss with antisense transcript activation.

260 TEs that are highly active in the absence of H1 and DNA methylation tend to show weak
261 upregulation when methylation alone is lost (Figures 5A and 5E). We therefore asked if antisense
262 intragenic transcription is analogously affected. Indeed, antisense transcription tends to behave
263 similarly in *met1* and *h1met1* (Figure 6J). Of particular interest, transcripts that are significantly
264 upregulated only in *h1met1* are usually also activated to some extent in *met1* (Figures 6J and S6B).
265 Thus, as with TEs, loss of H1 hyperactivates antisense transcripts that are released from silencing
266 by elimination of intragenic methylation.

267 **Discussion**

268 DNA methylation and histone H1 are abundant and widely conserved constituents of eukaryotic
269 chromatin associated with transcriptional inactivity (Fyodorov et al., 2018; Torres et al., 2016;
270 Zhang et al., 2018a), and their interactions have been of interest for many years. There is now
271 extensive evidence that H1 modulates DNA methylation pathways. Loss of H1 causes genome-
272 wide hypermethylation in ascomycete fungi (Barra et al., Mol Cell Biol 2000; Seymour, G3 2016)
273 and reduces methylation at specific loci in mouse (Fan et al., 2005; Geeven et al., 2015; MacLean
274 et al., 2011; Yang et al., 2013). In *Arabidopsis*, loss of H1 reduces methylation of euchromatic
275 TEs and increases methylation of heterochromatic elements in all sequence contexts (Rutowicz et
276 al., 2015; Zemach et al., 2013). H1 also appears to impede DNA demethylation in *Arabidopsis*
277 heterochromatin (He et al., 2018). H1 hinders heterochromatic methylation by restricting the
278 access of DNA methyltransferases (Lyons and Zilberman, 2017), and likely interferes with
279 demethylation in an analogous way. The ability of H1 to globally influence nucleosome positions
280 in plants (Figure 2) and animals (Baldi et al., 2018; Fan et al., 2003; Woodcock et al., 2006)
281 suggests an additional regulatory mechanism, because nucleosomes are substantial obstacles to
282 DNA methylation (Baubec et al., 2015; Huff and Zilberman, 2014; Lyons and Zilberman, 2017).

283 The effects of DNA methylation on H1 are far less established. A number of studies
284 evaluated whether H1 has preferential affinity for methylated DNA *in vitro* but came to opposing
285 conclusions (Campoy et al., 1995; Hashimshony et al., 2003; Levine et al., 1993; McArthur and
286 Thomas, 1996; Nightingale and Wolffe, 1995). Our results show that H1 is enriched at methylated
287 loci in *Arabidopsis*, but this enrichment does not depend on DNA methylation *in vivo* (Figure 1).
288 Our data indicate that the regulatory relationship between H1 and DNA methylation is

289 unidirectional: H1 modulates, but is not directly affected by, DNA methylation. However,
290 methylation indirectly influences H1 by, for example, enforcing TE silencing (Figure 1F).

291 The complex relationship between H1 and DNA methylation ultimately impinges on
292 chromatin accessibility and transcription. Our results indicate that H1 and DNA methylation
293 jointly maintain heterochromatic TEs in an inaccessible and silent state (Figure 5). Methylation is
294 the more powerful repressor, as few TEs are activated in *h1* mutants, and many of those that gain
295 activity also lose methylation (Figure 4). However, the role of H1 becomes obvious when
296 methylation is reduced, and loss of H1 can even overcome modest hypermethylation to activate
297 TEs (Figure 5E). These results may explain why H1 depletion has a far more drastic effect on TE
298 activity in *Drosophila* (Iwasaki et al., 2016; Lu et al., 2013), which lacks cytosine DNA
299 methylation (Raddatz et al., 2013; Zemach et al., 2010), than in mouse (Fan et al., 2005).

300 The cooperative silencing of transcription by methylation and H1 extends to gene bodies
301 (Figure 6). The function of gbM has been extensively debated for over a decade. One line of
302 argument is that gbM reprogramming regulates development (Herb et al., 2012), for example by
303 modulating alternative splicing (Lyko et al., 2010; Park et al., 2011). These ideas are supported by
304 developmental disruptions caused by erasure of methylation and/or downregulation of DNA
305 methyltransferases in species in which methylation is exclusive or near-exclusive to gene bodies
306 (Bewick et al., 2018; Biergans et al., 2017; Kucharski et al., 2008). However, in every species
307 examined so far, gbM is concentrated in constitutively expressed housekeeping genes (Coleman-
308 Derr and Zilberman, 2012; Dixon et al., 2016; Sarda et al., 2012; Zilberman, 2017). These genes
309 do not vary in expression during development and thus are not good candidates for differential
310 alternative splicing or other developmental regulation. There is also little evidence for substantial
311 shifts in gbM patterns during plant or animal development (Bartels et al., 2018; Libbrecht et al.,

312 2016; Suzuki et al., 2013; Zemach et al., 2018). Another argument is that gbM is a functionless
313 consequence of TE methylation (Bewick and Schmitz, 2017; Bewick et al., 2016; Teixeira and
314 Colot, 2009), motivated by the inability to detect transcriptional or RNA processing changes
315 caused by genetic removal of gbM. This argument is undermined by the well-established
316 observation that methylation is mutagenic in plants and animals (Alexandrov et al., 2013; Takuno
317 and Gaut, 2013). The maintenance of DNA methylation within the exons of some of the most
318 conserved and essential genes, especially in species that do not methylate other sequences, implies
319 a function that is important enough to outweigh the costs of increased mutation rates (Hunt et al.,
320 2013; Takuno and Gaut, 2013).

321 The last line of argument is that developmentally invariant methylation within
322 housekeeping genes should have one or more housekeeping functions (Zilberman, 2017). This is
323 supported by observations of small overall drops in gene expression associated with evolutionary
324 loss of gbM in plants (Muyle and Gaut, 2018; Takuno et al., 2017). One housekeeping function,
325 the inhibition of intragenic aberrant transcripts, was proposed when gbM was first discovered
326 (Tran et al., 2005). Mechanisms to silence such transcripts have been described in multiple species,
327 indicating that this is an important feature of transcriptional homeostasis (Carrozza et al., 2005;
328 Kaplan et al., 2003; Neri et al., 2017; Whitehouse et al., 2007). Here we provide the long-sought
329 experimental evidence for this gbM function. Our data show that intragenic antisense transcription
330 is upregulated in *h1met1* plants (Figure 6A). Most upregulated transcripts are anticorrelated with
331 sense expression (Figure 6D) and about half of these (55%) initiate from methylated DNA – far
332 more than is expected by random chance (Figure 6E). Conversely, antisense transcripts that initiate
333 from methylated DNA are preferentially upregulated in *h1met1* (Figure 6I). Antisense transcripts
334 activated in *h1met1* also tend to be upregulated, albeit more weakly, in *met1* (Figure 6J). Taken

335 together with the observed silencing of TEs by methylation and H1, the suppression of gene
336 transcription by H1, and the ability of H1 to associate with chromatin independently of DNA
337 methylation, our results strongly support the hypothesis that H1 and DNA methylation
338 cooperatively repress aberrant intragenic transcripts in *Arabidopsis*. The strong similarities
339 between gbM patterns of plants and animals (Feng et al., 2010; Zemach et al., 2010), and the
340 abundance of H1 in animal genes (Cao et al., 2013; Millán-Ariño et al., 2014), suggest that this
341 function is general, and potentially universal among eukaryotes with intragenic methylation.

342 **Acknowledgements**

343 We thank X. Feng, E. Hollwey and S. de-Bruijin for helpful comments on the manuscript. We also
344 thank S.L. McDevitt and M. Chung for sequencing and C. Wistrom for greenhouse assistance.
345 **Funding:** This work was supported by a fellowship from the Human Frontier Science Program
346 (LT000667/2013) and the National Research Foundation of Korea (2013022168) to J.C., by a
347 fellowship from the Helen Hay Whitney Foundation to D.B.L., by a European Research Council
348 grant (725746) and a Faculty Scholar grant from HHMI and the Simons Foundation (55108592)
349 to D.Z., and by the National Institutes of Health S10 program (1S10RR026866-01).

350 **Author contributions**

351 J.C. designed and performed experiments, analyzed data and wrote the manuscript. D.B.L.
352 performed cytology, image analysis, NRL calculation and MNase-seq analysis. M.Y.K. performed
353 H1 ChAP-seq experiments. J.D.M. defined the boundary of gbM regions. D.Z. conceived and
354 supervised the project and wrote the manuscript.

355 **Declaration of interests**

356 The authors declare no competing interests.

357
358

359 **References**

360 Alexandrov, L.B., Nik-Zainal, S., Wedge, D.C., Aparicio, S.A.J.R., Behjati, S., Biankin, A. V.,
361 Bignell, G.R., Bolli, N., Borg, A., Børresen-Dale, A.L., et al. (2013). Signatures of mutational
362 processes in human cancer. Nature *500*, 415–421.

363 Ascenzi, R., and Gantt, J.S. (1999). Subnuclear distribution of the entire complement of linker
364 histone variants in Arabidopsis thaliana. Chromosoma *108*, 345–355.

365 Baldi, S., Krebs, S., Blum, H., and Becker, P.B. (2018). Genome-wide measurement of local
366 nucleosome array regularity and spacing by nanopore sequencing. Nat. Struct. Mol. Biol. *25*,
367 894–901.

368 Bartels, A., Han, Q., Nair, P., Stacey, L., Gaynier, H., Mosley, M., Huang, Q.Q., Pearson, J.K.,
369 Hsieh, T.F., An, Y.Q.C., et al. (2018). Dynamic DNA methylation in plant growth and
370 development. Int. J. Mol. Sci. *19*, 2144.

371 Baubec, T., Colombo, D.F., Wirbelauer, C., Schmidt, J., Burger, L., Krebs, A.R., Akalin, A., and
372 Schübeler, D. (2015). Genomic profiling of DNA methyltransferases reveals a role for DNMT3B
373 in genic methylation. Nature *520*, 243–247.

374 Bewick, A.J., and Schmitz, R.J. (2017). Gene body DNA methylation in plants. Curr. Opin. Plant
375 Biol. *36*, 103–110.

376 Bewick, A.J., Ji, L., Niederhuth, C.E., Willing, E.-M., Hofmeister, B.T., Shi, X., Wang, L., Lu,
377 Z., Rohr, N.A., Hartwig, B., et al. (2016). On the origin and evolutionary consequences of gene
378 body DNA methylation. Proc. Natl. Acad. Sci. USA *113*, 9111–9116.

379 Bewick, A.J., Vogel, K.J., Moore, A.J., and Schmitz, R.J. (2017). Evolution of DNA methylation
380 across insects. Mol. Biol. Evol. *34*, 654–665.

381 Bewick, A.J., Sanchez, Z., Mckinney, E.C., Moore, A.J., Moore, P.J., and Schmitz, R.J. (2018).
382 Gene-regulatory independent functions for insect DNA methylation. BioRxiv 355669.

383 Biergans, S.D., Claudianos, C., Reinhard, J., and Galizia, C.G. (2017). DNA methylation
384 mediates neural processing after odor learning in the honeybee. Sci. Rep. *7*, 43635.

385 Bray, N.L., Pimentel, H., Melsted, P., and Pachter, L. (2016). Near-optimal probabilistic RNA-
386 seq quantification. Nat. Biotechnol. *34*, 525–527.

387 Burger, L., Gaidatzis, D., Schübeler, D., and Stadler, M.B. (2013). Identification of active
388 regulatory regions from DNA methylation data. Nucleic Acids Res. *41*, e155.

389 Campoy, F.J., Meehan, R.R., McKay, S., Nixon, J., and Bird, A. (1995). Binding of histone H1
390 to DNA is indifferent to methylation at CpG sequences. J. Biol. Chem. *270*, 26473–26481.

391 Cao, K., Lailler, N., Zhang, Y., Kumar, A., Uppal, K., Liu, Z., Lee, E.K., Wu, H., Medrzycki,
392 M., Pan, C., et al. (2013). High-Resolution Mapping of H1 Linker Histone Variants in

393 Embryonic Stem Cells. PLoS Genet. *9*, e1003417.

394 Carrozza, M.J., Li, B., Florens, L., Suganuma, T., Swanson, S.K., Lee, K.K., Shia, W.J.,
395 Anderson, S., Yates, J., Washburn, M.P., et al. (2005). Histone H3 methylation by Set2 directs
396 deacetylation of coding regions by Rpd3S to suppress spurious intragenic transcription. Cell *123*,
397 581–592.

398 Chambon, A., West, A., Vezon, D., Horlow, C., De Muyt, A., Chelysheva, L., Ronceret, A.,
399 Darbyshire, A.R., Osman, K., Heckmann, S., et al. (2018). Identification of ASYNAPTIC4, a
400 component of the meiotic chromosome axis. Plant Physiol. *178*, 233–246.

401 Chen, C., Li, C., Wang, Y., Renaud, J., Tian, G., Kambhampati, S., Saatian, B., Nguyen, V.,
402 Hannoufa, A., Marsolais, F., et al. (2017). Cytosolic acetyl-CoA promotes histone acetylation
403 predominantly at H3K27 in Arabidopsis. Nat. Plants *3*, 814–824.

404 Cheng, C.-Y., Krishnakumar, V., Chan, A.P., Thibaud-Nissen, F., Schobel, S., and Town, C.D.
405 (2017). Araport11: a complete reannotation of the *Arabidopsis thaliana* reference genome. Plant
406 J. *89*, 789–804.

407 Choi, K., Zhao, X., Tock, A.J., Lambing, C., Underwood, C.J., Hardcastle, T.J., Serra, H., Kim,
408 J., Cho, H.S., Kim, J., et al. (2018). Nucleosomes and DNA methylation shape meiotic DSB
409 frequency in Arabidopsis thaliana transposons and gene regulatory regions. Genome Res. *28*,
410 532–546.

411 Cokus, S.J., Feng, S., Zhang, X., Chen, Z., Merriman, B., Haudenschild, C.D., Pradhan, S.,
412 Nelson, S.F., Pellegrini, M., and Jacobsen, S.E. (2008). Shotgun bisulphite sequencing of the
413 Arabidopsis genome reveals DNA methylation patterning. Nature *452*, 215–219.

414 Coleman-Derr, D., and Zilberman, D. (2012). DNA methylation, H2A.Z, and the regulation of
415 constitutive expression. Cold Spring Harb. Symp. Quant. Biol. *77*, 147–154.

416 Davey, C., Pennings, S., and Allan, J. (1997). CpG methylation remodels chromatin structure in
417 vitro. J. Mol. Biol. *267*, 276–288.

418 Deaton, M., Webb, S., Kerr, A.R.W., Illingworth, R.S., Guy, J., Andrews, R., and Bird, A.
419 (2011). Cell type – specific DNA methylation at intragenic CpG islands in the immune system.
420 Genome Researh *21*, 1074–1086.

421 Deleris, A., Stroud, H., Bernatavichute, Y., Johnson, E., Klein, G., Schubert, D., and Jacobsen,
422 S.E. (2012). Loss of the DNA methyltransferase MET1 induces H3K9 hypermethylation at PcG
423 target genes and redistribution of H3K27 trimethylation to transposons in Arabidopsis thaliana.
424 PLoS Genet. *8*, e1003062.

425 Dixon, G.B., Bay, L.K., and Matz, M. V. (2016). Evolutionary consequences of DNA
426 methylation in a basal metazoan. Mol. Biol. Evol. *33*, 2285–2293.

427 Du, J., Johnson, L.M., Jacobsen, S.E., and Patel, D.J. (2015). DNA methylation pathways and
428 their crosstalk with histone methylation. Nat. Rev. Mol. Cell Biol. *16*, 519–532.

429 Fan, Y., Nikitina, T., Morin-Kensicki, E.M., Zhao, J., Magnuson, T.R., Woodcock, C.L., and
430 Skoultchi, A.I. (2003). H1 linker histones are essential for mouse development and affect
431 nucleosome spacing in vivo. Mol. Cell. Biol. *23*, 4559–4572.

432 Fan, Y., Nikitina, T., Zhao, J., Fleury, T.J., Bhattacharyya, R., Bouhassira, E.E., Stein, A.,
433 Woodcock, C.L., and Skoultchi, A.I. (2005). Histone H1 depletion in mammals alters global
434 chromatin structure but causes specific changes in gene regulation. Cell *123*, 1199–1212.

435 Feng, W., and Michaels, S.D. (2015). Accessing the inaccessible: The organization,
436 transcription, replication, and repair of heterochromatin in plants. Annu. Rev. Genet. *49*, 439–
437 459.

438 Feng, S., Cokus, S.J., Zhang, X., Chen, P.-Y., Bostick, M., Goll, M.G., Hetzel, J., Jain, J.,
439 Strauss, S.H., Halpern, M.E., et al. (2010). Conservation and divergence of methylation
440 patterning in plants and animals. Proc. Natl. Acad. Sci. USA *107*, 8689–8694.

441 Fransz, P., de Jong, J.H., Lysak, M., Castiglione, M.R., and Schubert, I. (2002). Interphase
442 chromosomes in Arabidopsis are organized as well defined chromocenters from which
443 euchromatin loops emanate. Proc. Natl. Acad. Sci. USA *99*, 14584–14589.

444 Fyodorov, D. V., Zhou, B.-R., Skoultchi, A.I., and Bai, Y. (2018). Emerging roles of linker
445 histones in regulating chromatin structure and function. Nat. Rev. Mol. Cell Biol. *19*, 192–206.

446 Geeven, G., Zhu, Y., Kim, B.J., Bartholdy, B.A., Yang, S.-M., Macfarlan, T.S., Gifford, W.D.,
447 Pfaff, S.L., Verstegen, M.J.A.M., Pinto, H., et al. (2015). Local compartment changes and
448 regulatory landscape alterations in histone H1-depleted cells. Genome Biol. *16*, 289.

449 Hashimshony, T., Zhang, J., Keshet, I., Bustin, M., and Cedar, H. (2003). The role of DNA
450 methylation in setting up chromatin structure during development. Nat. Genet. *34*, 187–192.

451 He, S., Vickers, M., Zhang, J., and Feng, X. (2018). Natural depletion of H1 in sex cells causes
452 DNA demethylation, heterochromatin decondensation and transposon activation. BioRxiv
453 451930.

454 Hellman, A., and Chess, A. (2007). Gene body–specific methylation on the active X
455 chromosome. Science *315*, 1141–1143.

456 Herb, B.R., Wolschin, F., Hansen, K.D., Aryee, M.J., Langmead, B., Irizarry, R., Amdam, G. V.,
457 and Feinberg, A.P. (2012). Reversible switching between epigenetic states in honeybee
458 behavioral subcastes. Nat. Neurosci. *15*, 1371–1373.

459 Hergeth, S.P., and Schneider, R. (2015). The H1 linker histones: multifunctional proteins beyond
460 the nucleosomal core particle. EMBO Rep. *16*, 1439–1453.

461 Hon, G.C., Rajagopal, N., Shen, Y., McCleary, D.F., Yue, F., Dang, M.D., and Ren, B. (2013).
462 Epigenetic memory at embryonic enhancers identified in DNA methylation maps from adult
463 mouse tissues. Nat. Genet. *45*, 1198–1206.

464 de Hoon, M.J.L., Imoto, S., Nolan, J., and Miyano, S. (2004). Open source clustering software.
465 Bioinformatics *20*, 1453–1454.

466 Huff, J.T., and Zilberman, D. (2014). Dnmt1-independent CG methylation contributes to
467 nucleosome positioning in diverse eukaryotes. Cell *156*, 1286–1297.

468 Hunt, B.G., Glastad, K.M., Yi, S. V., and Goodisman, M.A.D. (2013). Patterning and regulatory
469 associations of DNA methylation are mirrored by histone modifications in insects. Genome Biol.
470 Evol. *5*, 591–598.

471 Iurlaro, M., von Meyenn, F., and Reik, W. (2017). DNA methylation homeostasis in human and
472 mouse development. Curr. Opin. Genet. Dev. *43*, 101–109.

473 Iwasaki, Y.W., Murano, K., Ishizu, H., Shibuya, A., Iyoda, Y., Siomi, M.C., Siomi, H., and
474 Saito, K. (2016). Piwi modulates chromatin accessibility by regulating multiple factors including
475 histone H1 to repress transposons. Mol. Cell *63*, 408–419.

476 Johnson, C.A., Goddard, J.P., and Adams, R.L. (1995). The effect of histone H1 and DNA
477 methylation on transcription. Biochem. J. *305 (Pt 3)*, 791–798.

478 Jones, P.A. (2012). Functions of DNA methylation: islands, start sites, gene bodies and beyond.
479 Nat. Rev. Genet. *13*, 484–492.

480 Jones, P.A., Issa, J.P.J., and Baylin, S. (2016). Targeting the cancer epigenome for therapy. Nat.
481 Rev. Genet. *17*, 630–641.

482 Jühling, F., Kretzmer, H., Bernhart, S.H., Otto, C., Stadler, P.F., and Hoffmann, S. (2016).
483 metilene: fast and sensitive detection of differentially methylated regions from bisulfite
484 sequencing data. *26*, 256–262.

485 Kaplan, C.D., Laprade, L., and Winston, F. (2003). Transcription elongation factors repress
486 transcription inititaion from cryptic sites. Science *301*, 1096–1099.

487 Kawakatsu, T., Huang, S.C., Jupe, F., Sasaki, E., Schmitz, R.J., Urich, M.A., Castanon, R., Nery,
488 J.R., Barragan, C., He, Y., et al. (2016). Epigenomic diversity in a global collection of
489 Arabidopsis thaliana accessions. Cell *166*, 492–505.

490 Kawashima, T., and Berger, F. (2014). Epigenetic reprogramming in plant sexual reproduction.
491 Nat. Rev. Genet. *15*, 613–624.

492 Kim, D., Langmead, B., and Salzberg, S.L. (2015). HISAT: a fast spliced aligner with low
493 memory requirements. Nat. Methods *12*, 357–360.

494 Krishnakumar, R., Gamble, M.J., Frizzell, K.M., Berrocal, J.G., Kininis, M., and Kraus, W.L.
495 (2008). Reciprocal binding of PARP-1 and histone H1 at promoters specifies transcriptional
496 outcomes. Science *319*, 819–821.

497 Kucharski, R., Maleszka, J., Foret, S., and Maleszka, R. (2008). Nutritional control of

498 reproductive status in honeybees via DNA methylation. Science *319*, 1827–1831.

499 Kulis, M., Heath, S., Bibikova, M., Queirós, A.C., Navarro, A., Clot, G., Martínez-Trillos, A.,
500 Castellano, G., Brun-Heath, I., Pinyol, M., et al. (2012). Epigenomic analysis detects widespread
501 gene-body DNA hypomethylation in chronic lymphocytic leukemia. Nat. Genet. *44*, 1236–1242.

502 Langmead, B., Trapnell, C., Pop, M., and Salzberg, S.L. (2009). Ultrafast and memory-efficient
503 alignment of short DNA sequences to the human genome. Genome Biol. *10*, R25.

504 Law, J.A., and Jacobsen, S.E. (2010). Establishing, maintaining and modifying DNA
505 methylation patterns in plants and animals. Nat. Rev. Genet. *11*, 204–220.

506 Lev Maor, G., Yearim, A., and Ast, G. (2015). The alternative role of DNA methylation in
507 splicing regulation. Trends Genet. *31*, 274–280.

508 Levine, A., Yeivin, A., Ben-Asher, E., Aloni, Y., and Razin, A. (1993). Histone H1-mediated
509 inhibition of transcription initiation of methylated templates in vitro. J. Biol. Chem. *268*, 21754–
510 21759.

511 Libbrecht, R., Oxley, P.R., Keller, L., and Kronauer, D.J.C. (2016). Robust DNA methylation in
512 the clonal raider ant brain. Curr. Biol. *26*, 391–395.

513 Lister, R., O'Malley, R.C., Tonti-Filippini, J., Gregory, B.D., Berry, C.C., Millar, A.H., and
514 Ecker, J.R. (2008). Highly integrated single-base resolution maps of the epigenome in
515 Arabidopsis. Cell *133*, 523–536.

516 Lister, R., Pelizzola, M., Dowen, R.H., Hawkins, R.D., Hon, G., Tonti-Filippini, J., Nery, J.R.,
517 Lee, L., Ye, Z., Ngo, Q.-M., et al. (2009). Human DNA methylomes at base resolution show
518 widespread epigenomic differences. Nature *462*, 315–322.

519 Love, M.I., Huber, W., and Anders, S. (2014). Moderated estimation of fold change and
520 dispersion for RNA-seq data with DESeq2. Genome Biol. *15*, 550.

521 Lu, X., Wontakal, S.N., Emelyanov, A. V., Morcillo, P., Konev, A.Y., Fyodorov, D. V., and
522 Skoultchi, A.I. (2009). Linker histone H1 is essential for Drosophila development, the
523 establishment of pericentric heterochromatin, and a normal polytene chromosome structure.
524 Genes Dev. *23*, 452–465.

525 Lu, X., Wontakal, S.N., Kavi, H., Kim, B.J., Guzzardo, P.M., Emelyanov, A. V, Xu, N., Hannon,
526 G.J., Zavadil, J., Fyodorov, D. V, et al. (2013). Drosophila H1 regulates the genetic activity of
527 heterochromatin by recruitment of Su(var)3-9. Science *340*, 78–81.

528 Luo, C., Sidote, D.J., Zhang, Y., Kerstetter, R.A., Michael, T.P., and Lam, E. (2013). Integrative
529 analysis of chromatin states in Arabidopsis identified potential regulatory mechanisms for
530 natural antisense transcript production. Plant J. *73*, 77–90.

531 Lyko, F., Foret, S., Kucharski, R., Wolf, S., Falckenhayn, C., and Maleszka, R. (2010). The
532 honey bee epigenomes: Differential methylation of brain DNA in queens and workers. PLoS

533 Biol. *8*, e1000506.

534 Lyons, D.B., and Zilberman, D. (2017). DDM1 and Lsh remodelers allow methylation of DNA
535 wrapped in nucleosomes. Elife *6*, e30674.

536 MacLean, J.A., Bettegowda, A., Kim, B.J., Lou, C.-H., Yang, S.-M., Bhardwaj, A., Shanker, S.,
537 Hu, Z., Fan, Y., Eckardt, S., et al. (2011). The Rhox homeobox gene cluster is imprinted and
538 selectively targeted for regulation by histone H1 and DNA methylation. Mol. Cell. Biol. *31*,
539 1275–1287.

540 Maunakea, A.K., Nagarajan, R.P., Bilenky, M., Ballinger, T.J., D'Souza, C., Fouse, S.D.,
541 Johnson, B.E., Hong, C., Nielsen, C., Zhao, Y., et al. (2010). Conserved role of intragenic DNA
542 methylation in regulating alternative promoters. Nature *466*, 253–257.

543 Maunakea, A.K., Chepelev, I., Cui, K., and Zhao, K. (2013). Intragenic DNA methylation
544 modulates alternative splicing by recruiting MeCP2 to promote exon recognition. Cell Res. *23*,
545 1256–1269.

546 McArthur, M., and Thomas, J.O. (1996). A preference of histone H1 for methylated DNA.
547 EMBO J. *15*, 1705–1714.

548 Mercier, R., Mézard, C., Jenczewski, E., Macaisne, N., and Grelon, M. (2015). The Molecular
549 Biology of Meiosis in Plants. Annu. Rev. Plant Biol. *66*, 297–327.

550 Millán-Ariño, L., Islam, A.B.M.M.K., Izquierdo-Bouldstridge, A., Mayor, R., Terme, J.-M.,
551 Luque, N., Sancho, M., López-Bigas, N., and Jordan, A. (2014). Mapping of six somatic linker
552 histone H1 variants in human breast cancer cells uncovers specific features of H1.2. Nucleic
553 Acids Res. *42*, 4474–4493.

554 Morselli, M., Pastor, W.A., Montanini, B., Nee, K., Ferrari, R., Fu, K., Bonora, G., Rubbi, L.,
555 Clark, A.T., Ottonello, S., et al. (2015). In vivo targeting of de novo DNA methylation by
556 histone modifications in yeast and mouse. Elife *4*, e06205.

557 Muyle, A., and Gaut, B.S. (2018). Loss of gene body methylation in Eutrema salsugineum is
558 associated with reduced gene expression. Mol. Biol. Evol. doi: 10.1093/molbev/msy204.

559 Neri, F., Rapelli, S., Krepelova, A., Incarnato, D., Parlato, C., Basile, G., Maldotti, M., Anselmi,
560 F., and Oliviero, S. (2017). Intragenic DNA methylation prevents spurious transcription
561 initiation. Nature *543*, 72–77.

562 Nightingale, K., and Wolffe, A.P. (1995). Methylation at CpG sequences does not influence
563 histone H1 binding to a nucleosome including a Xenopus borealis 5 S rRNA gene. J. Biol. Chem.
564 *270*, 4197–4200.

565 Olmedo-Monfil, V., Durán-Figueroa, N., Arteaga-Vázquez, M., Demesa-Arévalo, E., Autran, D.,
566 Grimanelli, D., Slotkin, R.K., Martienssen, R.A., and Vielle-Calzada, J.P. (2010). Control of
567 female gamete formation by a small RNA pathway in Arabidopsis. Nature *464*, 628–632.

568 Over, R.S., and Michaels, S.D. (2014). Open and closed: The roles of linker histones in plants
569 and animals. Mol. Plant *7*, 481–491.

570 Park, J., Peng, Z., Zeng, J., Elango, N., Park, T., Wheeler, D., Werren, J.H., and Yi, S. V. (2011).
571 Comparative analyses of DNA methylation and sequence evolution using Nasonia genomes.
572 Mol. Biol. Evol. *28*, 3345–3354.

573 Pertea, M., Pertea, G.M., Antonescu, C.M., Chang, T.-C., Mendell, J.T., and Salzberg, S.L.
574 (2015). StringTie enables improved reconstruction of a transcriptome from RNA-seq reads. Nat.
575 Biotechnol. *33*, 290–295.

576 Pertea, M., Kim, D., Pertea, G.M., Leek, J.T., and Salzberg, S.L. (2016). Transcript-level
577 expression analysis of RNA-seq experiments with HISAT, StringTie and Ballgown. Nat. Protoc.
578 *11*, 1650–1667.

579 Pimentel, H., Bray, N.L., Puente, S., Melsted, P., and Pachter, L. (2017). Differential analysis of
580 RNA-seq incorporating quantification uncertainty. Nat. Methods *14*, 687–690.

581 Quinlan, A.R., and Hall, I.M. (2010). BEDTools: a flexible suite of utilities for comparing
582 genomic features. Bioinformatics *26*, 841–842.

583 Raddatz, G., Guzzardo, P.M., Olova, N., Fantappie, M.R., Rampp, M., Schaefer, M., Reik, W.,
584 Hannon, G.J., and Lyko, F. (2013). Dnmt2-dependent methylomes lack defined DNA
585 methylation patterns. Proc. Natl. Acad. Sci. USA *110*, 8627–8631.

586 Ramírez, F., Ryan, D.P., Grüning, B., Bhardwaj, V., Kilpert, F., Richter, A.S., Heyne, S.,
587 Dündar, F., and Manke, T. (2016). deepTools2: a next generation web server for deep-
588 sequencing data analysis. Nucleic Acids Res. *44*, W160–W165.

589 Rasmussen, K.D., and Helin, K. (2016). Role of TET enzymes in DNA methylation,
590 development, and cancer. Genes Dev. *30*, 733–750.

591 Regulski, M., Lu, Z., Kendall, J., Donoghue, M.T.A., Reinders, J., Llaca, V., Deschamps, S.,
592 Smith, A., Levy, D., McCombie, W.R., et al. (2013). The maize methylome influences mRNA
593 splice sites and reveals widespread paramutation-like switches guided by small RNA. Genome
594 Res. *23*, 1651–1662.

595 Robertson, K.D. (2005). DNA methylation and human disease. Nat. Rev. Genet. *6*, 597–610.

596 Robinson, J.T., Thorvaldsdóttir, H., Winckler, W., Guttman, M., Lander, E.S., Getz, G., and
597 Mesirov, J.P. (2011). Integrative genomics viewer. Nat. Biotechnol. *29*, 24–26.

598 Rutowicz, K., Puzio, M., Halibart-Puzio, J., Lirski, M., Kotliński, M., Kroteń, M.A., Knizewski,
599 L., Lange, B., Muszewska, A., Śniegowska-Świerk, K., et al. (2015). A specialized histone H1
600 variant is required for adaptive responses to complex abiotic stress and related DNA methylation
601 in Arabidopsis. Plant Physiol. *169*, 2080–2101.

602 Sarda, S., Zeng, J., Hunt, B.G., and Yi, S. V. (2012). The evolution of invertebrate gene body

603 methylation. Mol. Biol. Evol. *29*, 1907–1916.

604 Schindelin, J., Arganda-Carreras, I., Frise, E., Kaynig, V., Longair, M., Pietzsch, T., Preibisch,
605 S., Rueden, C., Saalfeld, S., Schmid, B., et al. (2012). Fiji: an open-source platform for
606 biological-image analysis. Nat. Methods *9*, 676–682.

607 Schmidt, A., Schmid, M.W., and Grossniklaus, U. (2015). Plant germline formation: common
608 concepts and developmental flexibility in sexual and asexual reproduction. Development *142*,
609 229–241.

610 Schmitz, R.J., Schultz, M.D., Lewsey, M.G., O'Malley, R.C., Urich, M.A., Libiger, O., Schork,
611 N.J., Ecker, J.R., and Epigenetic (2011). Transgenerational epigenetic instability is a source of
612 novel methylation variants. Science *334*, 369–373.

613 Schübeler, D. (2015). Function and information content of DNA methylation. Nature *517*, 321–
614 326.

615 She, W., and Baroux, C. (2015). Chromatin dynamics in pollen mother cells underpin a common
616 scenario at the somatic-to-reproductive fate transition of both the male and female lineages in
617 Arabidopsis. Front. Plant Sci. *6*, Article 294.

618 She, W., Grimanelli, D., Rutowicz, K., Whitehead, M.W.J., Puzio, M., Kotliński, M.,
619 Jerzmanowski, A., and Baroux, C. (2013). Chromatin reprogramming during the somatic-to-
620 reproductive cell fate transition in plants. Development *140*, 4008–4019.

621 Shukla, S., Kavak, E., Gregory, M., Imashimizu, M., Shutinoski, B., Kashlev, M., Oberdoerffer,
622 P., Sandberg, R., and Oberdoerffer, S. (2011). CTCF-promoted RNA polymerase II pausing links
623 DNA methylation to splicing. Nature *479*, 74–79.

624 Simpson, R.T. (1978). Structure of the chromatosome, a chromatin particle containing 160 base
625 pairs of DNA and all the histones. Biochemistry *17*, 5524–5531.

626 Smith, Z.D., and Meissner, A. (2013). DNA methylation: Roles in mammalian development.
627 Nat. Rev. Genet. *14*, 204–220.

628 Stempor, P., and Ahringer, J. (2016). SeqPlots - Interactive software for exploratory data
629 analyses, pattern discovery and visualization in genomics. Wellcome Open Res. *1*, 14.

630 Suzuki, M.M., and Bird, A. (2008). DNA methylation landscapes: provocative insights from
631 epigenomics. Nat. Rev. Genet. *9*, 465–476.

632 Suzuki, M.M., Kerr, A.R.W., De Sousa, D., and Bird, A. (2007). CpG methylation is targeted to
633 transcription units in an invertebrate genome. Genome Res. *17*, 625–631.

634 Suzuki, S., Shaw, G., and Renfree, M.B. (2013). Postnatal epigenetic reprogramming in the
635 germline of a marsupial, the tammar wallaby. Epigenetics and Chromatin *6*, 14.

636 Takuno, S., and Gaut, B.S. (2012). Body-methylated genes in Arabidopsis thaliana are

637 functionally important and evolve slowly. Mol. Biol. Evol. *29*, 219–227.

638 Takuno, S., and Gaut, B.S. (2013). Gene body methylation is conserved between plant orthologs
639 and is of evolutionary consequence. Proc. Natl. Acad. Sci. USA *110*, 1797–1802.

640 Takuno, S., Seymour, D.K., and Gaut, B.S. (2017). The evolutionary dynamics of orthologs that
641 shift in gene body methylation between Arabidopsis species. Mol. Biol. Evol. *34*, 1479–1491.

642 Teissandier, A., and Bourc'his, D. (2017). Gene body DNA methylation conspires with
643 H3K36me3 to preclude aberrant transcription. EMBO J. *36*, 1471–1473.

644 Teixeira, F.K., and Colot, V. (2009). Gene body DNA methylation in plants: a means to an end
645 or an end to a means? EMBO J. *28*, 997–998.

646 Thorvaldsdottir, H., Robinson, J.T., and Mesirov, J.P. (2013). Integrative Genomics Viewer
647 (IGV): high-performance genomics data visualization and exploration. Brief. Bioinform. *14*,
648 178–192.

649 To, T.K., Saze, H., and Kakutani, T. (2015). DNA Methylation within transcribed regions. Plant
650 Physiol. *168*, 1219–1225.

651 Torres, C.M., Biran, A., Burney, M.J., Patel, H., Henser-Brownhill, T., Cohen, A.-H.S., Li, Y.,
652 Ben-Hamo, R., Nye, E., Spencer-Dene, B., et al. (2016). The linker histone H1.0 generates
653 epigenetic and functional intratumor heterogeneity. Science *353*, aaf1644.

654 Tran, R.K., Henikoff, J.G., Zilberman, D., Ditt, R.F., Jacobsen, S.E., and Henikoff, S. (2005).
655 DNA methylation profiling identifies CG methylation clusters in Arabidopsis genes. Curr. Biol.
656 *15*, 154–159.

657 Valouev, A., Johnson, S.M., Boyd, S.D., Smith, C.L., Fire, A.Z., and Sidow, A. (2011).
658 Determinants of nucleosome organization in primary human cells. Nature *474*, 516–520.

659 Wagner, E.J., and Carpenter, P.B. (2012). Understanding the language of Lys36 methylation at
660 histone H3. Nat. Rev. Mol. Cell Biol. *13*, 115–126.

661 Whitehouse, I., Rando, O.J., Delrow, J., and Tsukiyama, T. (2007). Chromatin remodelling at
662 promoters suppresses antisense transcription. Nature *450*, 1031–1035.

663 Wierzbicki, A.T., and Jerzmanowski, A. (2005). Suppression of histone H1 genes in Arabidopsis
664 results in heritable developmental defects and stochastic changes in DNA methylation. Genetics
665 *169*, 997–1008.

666 Woodcock, C.L., Skoultchi, A.I., and Fan, Y. (2006). Role of linker histone in chromatin
667 structure and function: H1 stoichiometry and nucleosome repeat length. Chromosom. Res. *14*,
668 17–25.

669 Xiao, W., Gehring, M., Choi, Y., Margossian, L., Pu, H., Harada, J.J., Goldberg, R.B., Pennell,
670 R.I., and Fischer, R.L. (2003). Imprinting of the MEA polycomb gene is controlled by

671 antagonism between MET1 methyltransferase and DME glycosylase. Dev. Cell *5*, 891–901.

672 Yang, S.-M., Kim, B.J., Norwood Toro, L., and Skoultchi, A.I. (2013). H1 linker histone
673 promotes epigenetic silencing by regulating both DNA methylation and histone H3 methylation.
674 Proc. Natl. Acad. Sci. USA *110*, 1708–1713.

675 Yang, X., Han, H., De Carvalho, D.D., Lay, F.D., Jones, P.A., and Liang, G. (2014). Gene body
676 methylation can alter gene expression and is a therapeutic target in cancer. Cancer Cell *26*, 577–
677 590.

678 Yelagandula, R., Stroud, H., Holec, S., Zhou, K., Feng, S., Zhong, X., Muthurajan, U.M., Nie,
679 X., Kawashima, T., Groth, M., et al. (2014). The histone variant H2A.W defines heterochromatin
680 and promotes chromatin condensation in Arabidopsis. Cell *158*, 98–109.

681 Zemach, A., and Zilberman, D. (2010). Evolution of eukaryotic DNA methylation and the
682 pursuit of safer sex. Curr. Biol. *20*, R780–R785.

683 Zemach, A., McDaniel, I.E., Silva, P., and Zilberman, D. (2010). Genome-wide evolutionary
684 analysis of eukaryotic DNA methylation. Science *328*, 916–919.

685 Zemach, A., Kim, M.Y., Hsieh, P.-H., Coleman-Derr, D., Eshed-Williams, L., Thao, K., Harmer,
686 S.L., and Zilberman, D. (2013). The Arabidopsis nucleosome remodeler DDM1 allows DNA
687 methyltransferases to access H1-containing heterochromatin. Cell *153*, 193–205.

688 Zemach, A., Lloyd, J.P.B., Harris, K.D., and Zilberman, D. (2018). Maximum DNA Methylation
689 Fidelity in the Germline Tolerates Global Non-Functional Gene Body Methylation Dynamics
690 During Development. SSRN Electron. J.

691 Zhang, H., Lang, Z., and Zhu, J.-K. (2018a). Dynamics and function of DNA methylation in
692 plants. Nat. Rev. Mol. Cell Biol. *19*, 489–506.

693 Zhang, T., Zhang, W., and Jiang, J. (2015). Genome-wide nucleosome occupancy and
694 positioning and their impact on gene expression and evolution in plants. Plant Physiol. *168*,
695 1406–1416.

696 Zhang, Y., Harris, C.J., Liu, Q., Liu, W., Ausin, I., Long, Y., Xiao, L., Feng, L., Chen, X., Xie,
697 Y., et al. (2018b). Large-scale comparative epigenomics reveals hierarchical regulation of non-
698 CG methylation in Arabidopsis. Proc. Natl. Acad. Sci. USA E1069–E1074.

699 Zilberman, D. (2017). An evolutionary case for functional gene body methylation in plants and
700 animals. Genome Biol. *18*, 87.

701 Zilberman, D., Gehring, M., Tran, R.K., Ballinger, T., and Henikoff, S. (2007). Genome-wide
702 analysis of Arabidopsis thaliana DNA methylation uncovers an interdependence between
703 methylation and transcription. Nat. Genet. *39*, 61–69.

704 Zilberman, D., Coleman-Derr, D., Ballinger, T., and Henikoff, S. (2008). Histone H2A.Z and
705 DNA methylation are mutually antagonistic chromatin marks. Nature *456*, 125–129.

706 **Figure Legends**

707 **Figure 1. Histone H1 is enriched in methylated DNA independently of methylation. (A)**
708 Average H1.1 distribution around well-positioned nucleosomes. **(B)** Average H1.1, predicted H1,
709 and CG methylation (mCG) levels are plotted in 50 kb windows along *Arabidopsis* chromosome
710 4. **(C)** Box plots of H1.1 levels in heterochromatic TEs (hTEs), euchromatic TEs (eTEs), and genes.
711 The shaded area marks the middle 50% of genomic H1.1 levels. **(D)** H1.1 distribution around genes
712 with different expression levels. **(E)** Box plots of H1.1 abundance and predicted H1 abundance in
713 methylated (m) and unmethylated (u) genes in *wt* and *met1* plants. ** is $p < 0.01$, *** is $p < 0.001$,
714 **** is $p < 0.0001$, Student's *t*-test. **(F)** Heat maps of indicated chromatin features and expression
715 in MET1-independent and dependent hTEs. **(G)** Average H1.1 levels of 1 kb windows in *wt* and
716 *met1*. 1000 windows were randomly selected for plotting. "*r*" is Pearson's correlation coefficient.
717 **(H)** Principal component analysis of H1.1, H1.2, histone H3 lysine modifications, histone variant
718 H2A.W, DNA methylation (mCG, mCHG, mCHH), GC content (gc) and gene expression (exp).
719 **(I)** Linear model prediction of H1 distribution around the transcriptional start sites (TSS) of genes
720 in comparison to actual H1.1 distribution. **(J)** Example of actual H1.1 and predicted H1 distribution
721 at gene-body methylated genes in *wt* and *met1*. **(C and E)** Whiskers indicate 1.5X interquartile
722 range (IQR).

723

724 **Figure 2. Loss of H1 alters nucleosome organization. (A)** Nucleosome repeat length (NRL)
725 calculations for two biological replicates at genes grouped by their expression in *wt*. Phasograms
726 and linear regressions for the positions of nucleosome peaks at the genes with lowest expression
727 (shaded area) are in Figure S2A. **(B and E)** NRL calculations for two biological replicates at genes
728 (B) and TEs (E) grouped by H1 enrichment. **(C and F)** Phasograms and linear regressions for the

729 positions of nucleosome peaks at H1-rich genes (C) and TEs (F). **(D)** NRL calculations for two
730 biological replicates at TEs grouped by their H3K9me2 level in *wt*. Phasograms and linear
731 regressions for the positions of nucleosome peaks at H3K9me2-rich TEs (shaded area) are in
732 Figure S2B. **(A-B and D-E)** Error bars indicate standard error.
733
734 **Figure 3. Loss of H1 activates H1-rich meiosis-related genes. (A)** Number of up- and down-
735 regulated genes in *h1* plants vs. *wt*. **(B)** Heat maps of respective gene expression fold change vs.
736 *wt* in *h1* plants in leaves (L) and seedlings (S). Adjusted *p*-values for the expression change are
737 shown. **(C)** Box plots of *wt* H1 levels in genes upregulated (up), down-regulated (dn) and
738 unchanged (control; ct) in *h1* plants. "a" and "b" are significantly different ($p < 0.01$; ANOVA).
739 Whiskers indicate 1.5X IQR. **(D)** Distribution of H1 around control, up- and down-regulated genes.
740 Shaded areas represent 95% confidence intervals. **(E)** Violin plots of gene expression in *wt* plants
741 for control (ct), up- and down (dn)-regulated genes in (A). **(F)** An example meiosis-related gene
742 transcriptionally activated in *h1* plants. The dashed red line indicates average H1 level at genes.
743
744 **Figure 4. Loss of H1 disperses heterochromatin and weakly activates TEs. (A)** Nuclei of *wt*
745 and *h1* plants stained with DAPI. DAPI puncta volumes are highlighted in yellow. **(B)** Number
746 per nucleus and volume of DAPI puncta in *wt* and *h1* plants. Note that blurred chromocenter
747 boundaries in *h1* mutants cause some to be assigned very large volumes. The number of nuclei
748 (left) and DAPI puncta (right) used to generate the data were indicated. **(C)** Heat maps of
749 expression in leaves (L) and seedlings (S) with corresponding FDR (*h1* vs. *wt*) and TSS-proximal
750 DNA methylation change of TEs in *h1* plants vs. *wt*. *p*-value for methylation change was calculated
751 with Fisher's exact test. **(D)** Examples of upregulated TEs in *h1* plants. Note DNA methylation

752 loss near TSS (highlighted in yellow). **(E)** An example of upregulated TE in *h1* plants without
753 DNA methylation loss near TSS (highlighted in yellow). **(F)** Box plots of DNA accessibility of
754 hTEs, eTEs, and genes in *wt* and *h1*. Whiskers indicate 1.5X IQR.
755
756 **Figure 5. DNA methylation and H1 cooperatively silence TE expression. (A and E)** Expression,
757 TSS-proximal DNA methylation and DNA accessibility of hTEs in *wt*, *met1* and *h1met1* plants.
758 TEs with unchanged TSS non-CG methylation in *h1met1* compared to *met1* are shown in (A) and
759 TEs with altered non-CG methylation at the TSS are shown in (E). **(B and F)** Average CHG and
760 CHH methylation around TEs in the up1 (B) and up3 (F) clusters. Methylation from the TSS-
761 proximal regions shaded in yellow is shown in (A) and (E). **(C-D)** Box plots of *met1* H1 abundance
762 (C) and H1 distribution (D) in TEs in the nc and up1 clusters from (A). H1 from the TSS-proximal
763 region shaded in yellow in (D) is shown in (C). **** is $p < 0.0001$, Student's *t*-test. **(G-H)** Box
764 plots of *met1* H1 abundance (G) and H1 distribution (H) in TEs in the dn and up3 clusters from
765 (E). H1 from the TSS-proximal region shaded in yellow in (H) is shown in (G). *** is $p < 0.001$,
766 Student's *t*-test. **(C and G)** Whiskers indicate 1.5X IQR.
767
768 **Figure 6. DNA methylation and H1 cooperatively suppress intragenic antisense transcripts.**
769 **(A)** Number of differentially expressed antisense (AS) transcripts in *h1, met1,* and *h1met1* plants.
770 **(B and D)** Heat maps showing *wt* CG methylation at antisense TSS and expression of sense (S)
771 and antisense transcripts in *met1* (B) or *h1met1* (D) plants. **(C and E)** Box plots of TSS-proximal
772 *wt* CG methylation levels of upregulated (up) and downregulated (dn) antisense transcripts either
773 positively correlated (+) or negatively/un-correlated (0/-) with sense expression in *met1* (C) or
774 *h1met1* (E) plants. Data are also shown for unchanged (control; ct) antisense transcripts. Magenta

775 asterisks indicate the percentage of antisense TSS that overlap gbM. “a”, “b” and “c” are signi-
776 ficantly different; overlapping letters – i.e. “b” and “bc” – indicate that the difference is not
777 significant ($p < 0.01$; ANOVA). **(F)** *Wt* CG methylation around antisense TSS of indicated groups
778 from (E) with more than 100 transcripts. Shaded areas represent 95% confidence intervals. **(G-H)**
779 CG methylation (G) and H1.1 distribution (H) around the TSS of antisense transcripts initiated
780 from unmethylated genes, unmethylated regions within gbM genes, and methylated regions within
781 gbM genes. **(I)** Box plots of antisense expression in indicated groups from (G) in *met1* and *h1met1*
782 plants. “a”, “b” and “c” are significantly different ($p < 0.01$; ANOVA). **(J)** Heat maps of *wt* CG
783 methylation at antisense TSS, expression of sense and antisense transcripts compared to *wt*, and
784 corresponding antisense expression *p*-values in *met1* and *h1met1* plants. **(C, E and I)** Whiskers
785 indicate 1.5X IQR.

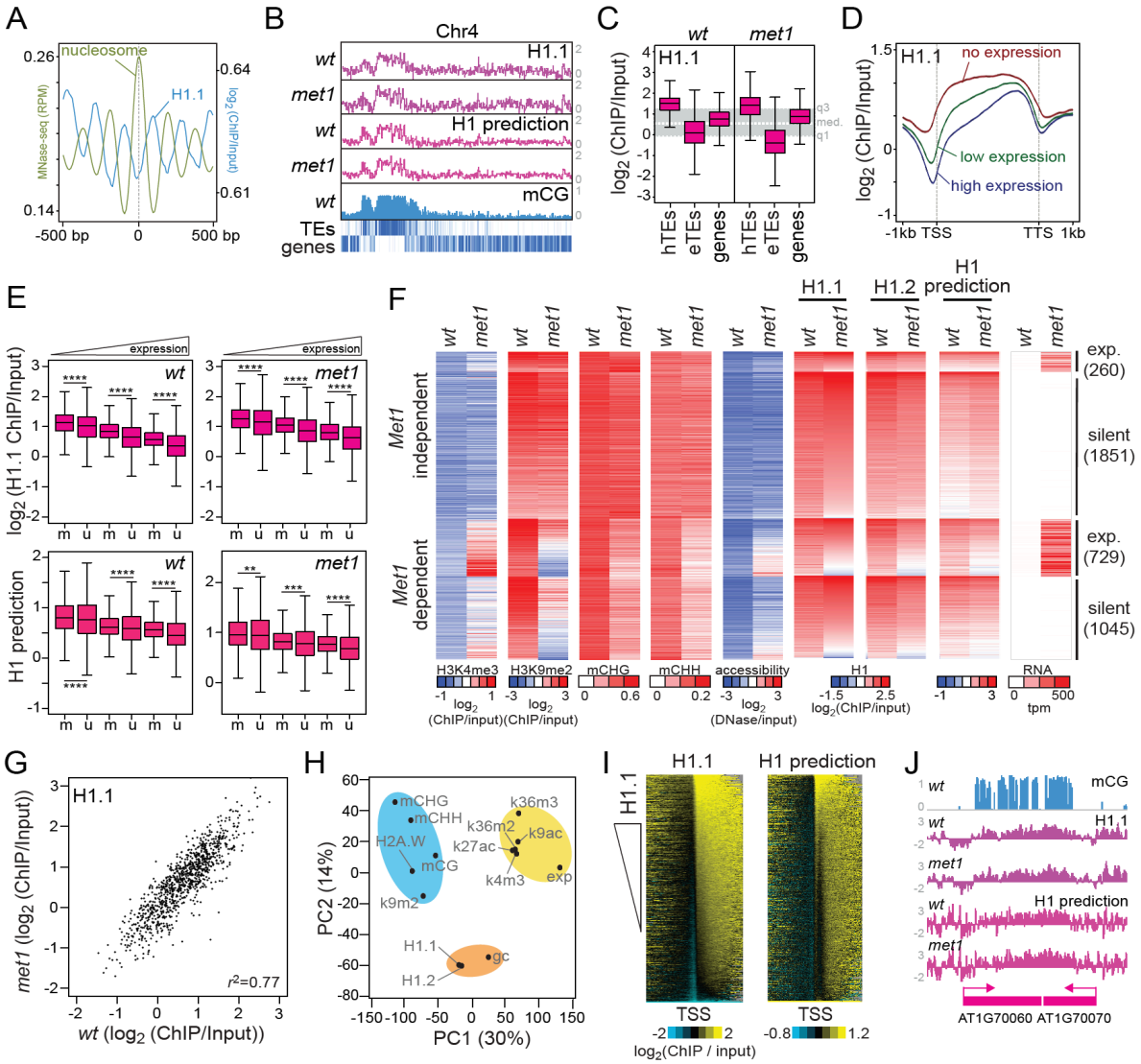

Figure 1. Histone H1 is enriched in methylated DNA independently of methylation. (A) Average H1.1 distribution around well-positioned nucleosomes. **(B)** Average H1.1, predicted H1, and CG methylation (mCG) levels are plotted in 50 kb windows along *Arabidopsis* chromosome 4. **(C)** Box plots of H1.1 levels in heterochromatic TEs (hTEs), euchromatic TEs (eTEs), and genes. The shaded area marks the middle 50% of genomic H1.1 levels. **(D)** H1.1 distribution around genes with different expression levels. **(E)** Box plots of H1.1 abundance and predicted H1 abundance in methylated (m) and unmethylated (u) genes in *wt* and *met1* plants. ** is $p < 0.01$, *** is $p < 0.001$, **** is $p < 0.0001$, Student's *t*-test. **(F)** Heat maps of indicated chromatin features and expression in MET1-independent and dependent hTEs. **(G)** Average H1.1 levels of 1 kb windows in *wt* and *met1*. 1000 windows were randomly selected for plotting. "*r*" is Pearson's correlation coefficient. **(H)** Principal component analysis of H1.1, H1.2, histone H3 lysine modifications, histone variant H2A.W, DNA methylation (mCG, mCHG, mCHH), GC content (gc) and gene expression (exp). **(I)** Linear model prediction of H1 distribution around the transcriptional start sites (TSS) of genes in comparison to actual H1.1 distribution. **(J)** Example of actual H1.1 and predicted H1 distribution at gene-body methylated genes in *wt* and *met1*. **(C and E)** Whiskers indicate 1.5X interquartile range (IQR).

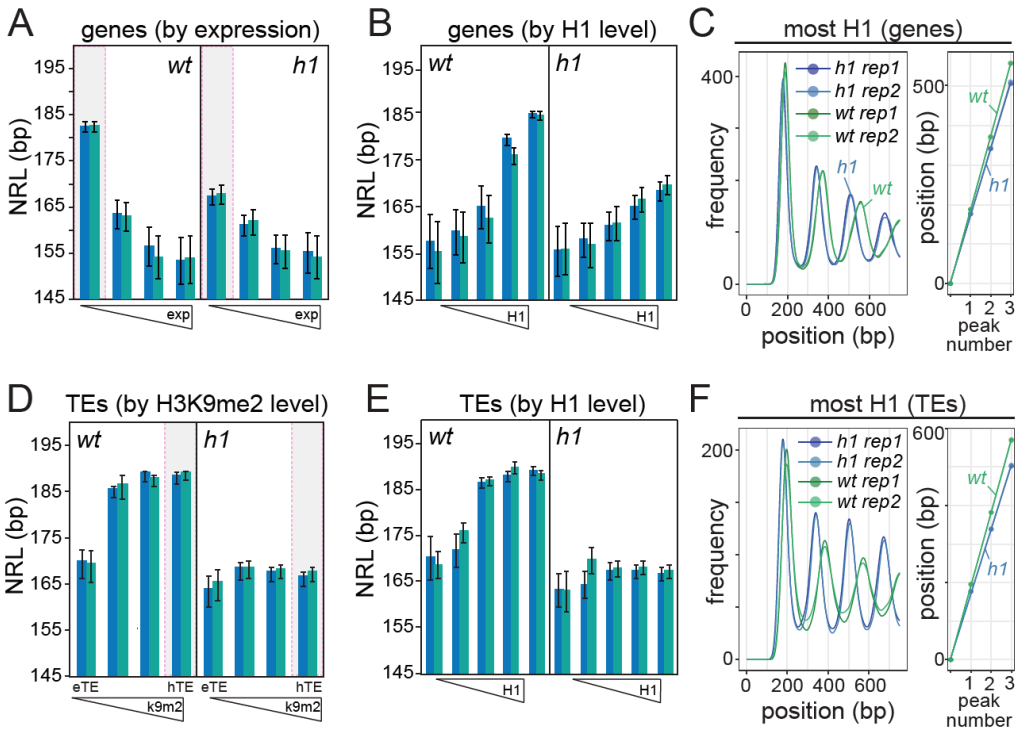

802 **Figure 2. Loss of H1 alters nucleosome organization. (A)** Nucleosome repeat length (NRL)
803 calculations for two biological replicates at genes grouped by their expression in *wt*. Phasograms
804 and linear regressions for the positions of nucleosome peaks at the genes with lowest expression
805 (shaded area) are in Figure S2A. **(B and E)** NRL calculations for two biological replicates at genes
806 (B) and TEs (E) grouped by H1 enrichment. **(C and F)** Phasograms and linear regressions for the
807 positions of nucleosome peaks at H1-rich genes (C) and TEs (F). **(D)** NRL calculations for two
808 biological replicates at TEs grouped by their H3K9me2 level in *wt*. Phasograms and linear
809 regressions for the positions of nucleosome peaks at H3K9me2-rich TEs (shaded area) are in
810 Figure S2B. **(A-B and D-E)** Error bars indicate standard error.

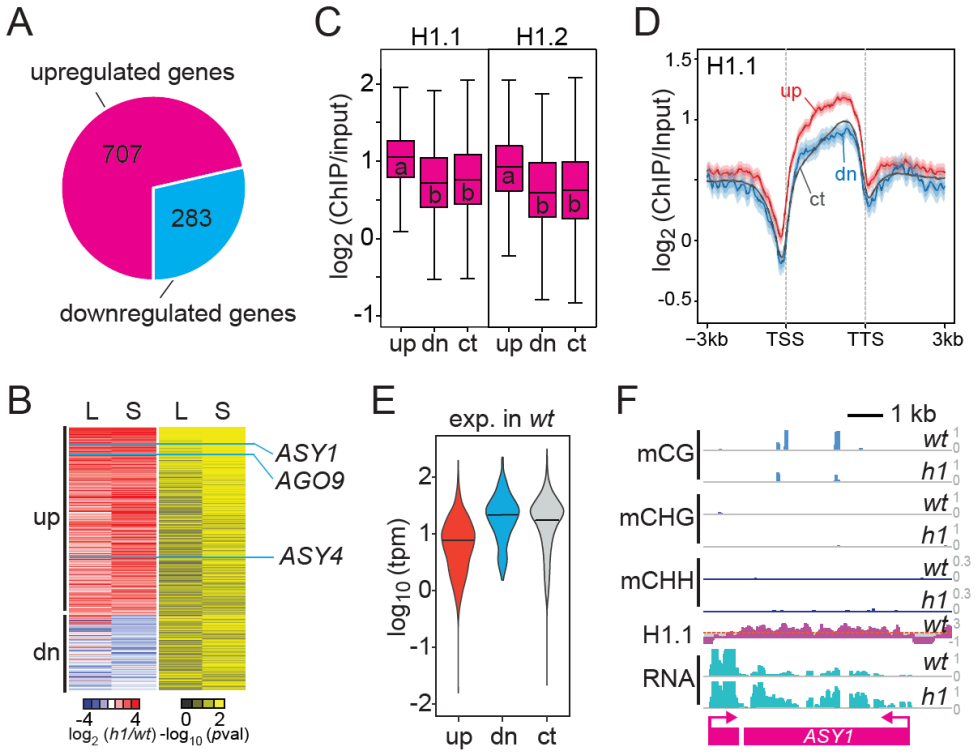

Figure 3. Loss of H1 activates H1-rich meiosis-related genes. (A) Number of up- and down-regulated genes in *h1* plants vs. *wt*. **(B)** Heat maps of respective gene expression fold change vs. *wt* in *h1* plants in leaves (L) and seedlings (S). Adjusted *p*-values for the expression change are shown. **(C)** Box plots of *wt* H1 levels in genes upregulated (up), down-regulated (dn) and unchanged (control; ct) in *h1* plants. "a" and "b" are significantly different ($p < 0.01$; ANOVA). Whiskers indicate 1.5X IQR. **(D)** Distribution of H1 around control, up- and down-regulated genes. Shaded areas represent 95% confidence intervals. **(E)** Violin plots of gene expression in *wt* plants for control (ct), up- and down (dn)-regulated genes in (A). **(F)** An example meiosis-related gene transcriptionally activated in *h1* plants. The dashed red line indicates average H1 level at genes.

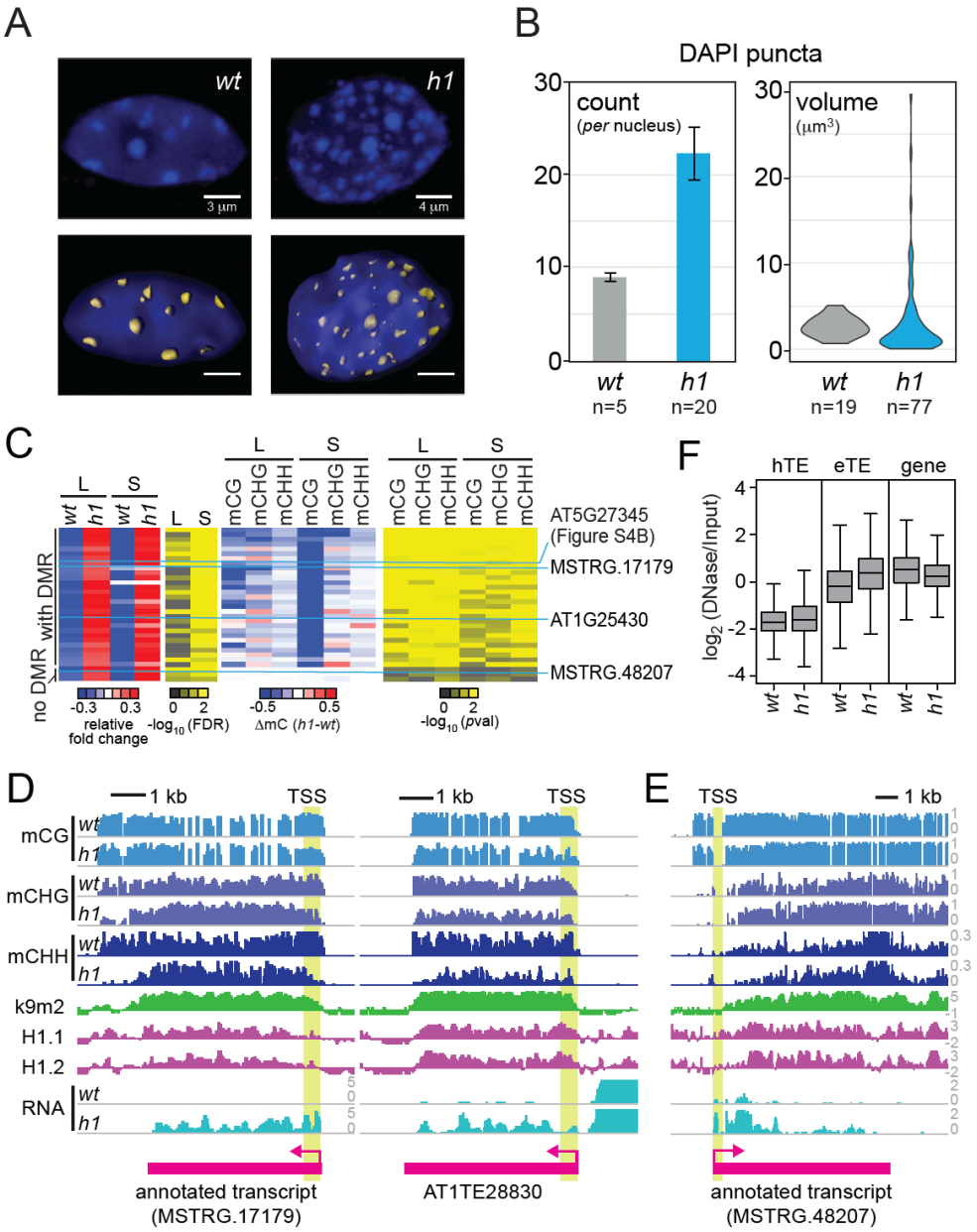

Figure 4. Loss of H1 disperses heterochromatin and weakly activates TEs. (A) Nuclei of *wt* and *h1* plants stained with DAPI. DAPI puncta volumes are highlighted in yellow. **(B)** Number per nucleus and volume of DAPI puncta in *wt* and *h1* plants. Note that blurred chromocenter boundaries in *h1* mutants cause some to be assigned very large volumes. The number of nuclei (left) and DAPI puncta (right) used to generate the data were indicated. **(C)** Heat maps of expression in leaves (L) and seedlings (S) with corresponding FDR (*h1* vs. *wt*) and TSS-proximal DNA methylation change of TEs in *h1* plants vs. *wt*. *p*-value for methylation change was calculated with Fisher's exact test. **(D)** Examples of upregulated TEs in *h1* plants. Note DNA methylation loss near TSS (highlighted in yellow). **(E)** An example of upregulated TE in *h1* plants without DNA methylation loss near TSS (highlighted in yellow). **(F)** Box plots of DNA accessibility of hTEs, eTEs, and genes in *wt* and *h1*. Whiskers indicate 1.5X IQR.

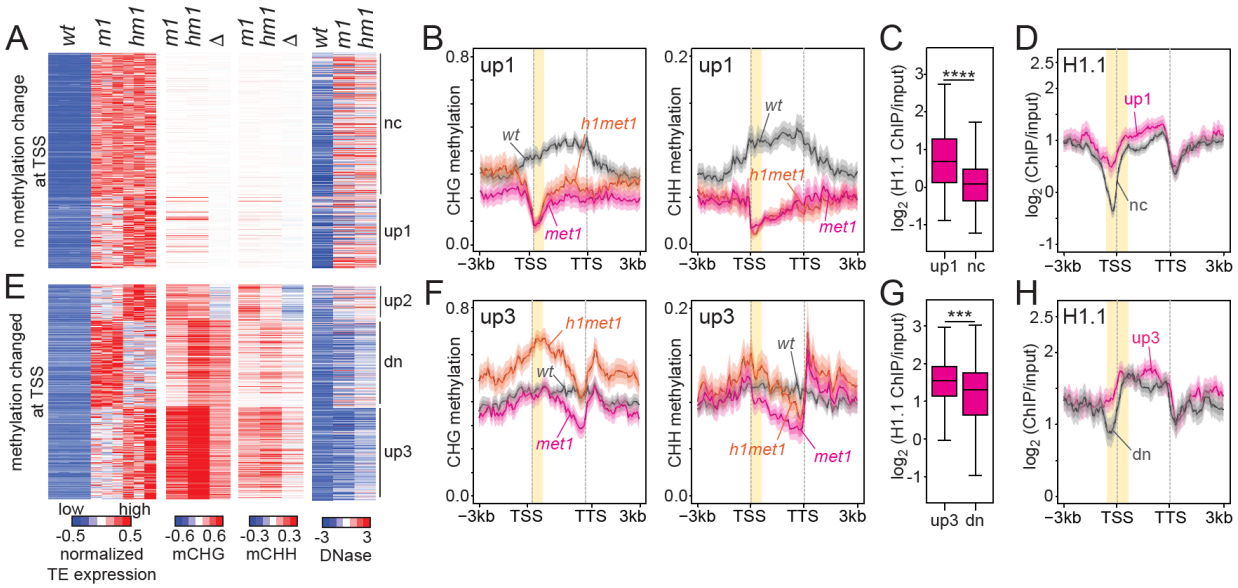

Figure 5. DNA methylation and H1 cooperatively silence TE expression. (A and E) Expression, TSS-proximal DNA methylation and DNA accessibility of hTEs in *wt*, *met1* and *h1met1* plants. TEs with unchanged TSS non-CG methylation in *h1met1* compared to *met1* are shown in (A) and TEs with altered non-CG methylation at the TSS are shown in (E). **(B and F)** Average CHG and CHH methylation around TEs in the up1 (B) and up3 (F) clusters. Methylation from the TSS-proximal regions shaded in yellow is shown in (A) and (E). **(C-D)** Box plots of *met1* H1 abundance (C) and H1 distribution (D) in TEs in the nc and up1 clusters from (A). H1 from the TSS-proximal region shaded in yellow in (D) is shown in (C). **** is $p < 0.0001$, Student's *t*-test. **(G-H)** Box plots of *met1* H1 abundance (G) and H1 distribution (H) in TEs in the dn and up3 clusters from (E). H1 from the TSS-proximal region shaded in yellow in (H) is shown in (G). *** is $p < 0.001$, Student's *t*-test. **(C and G)** Whiskers indicate 1.5X IQR.

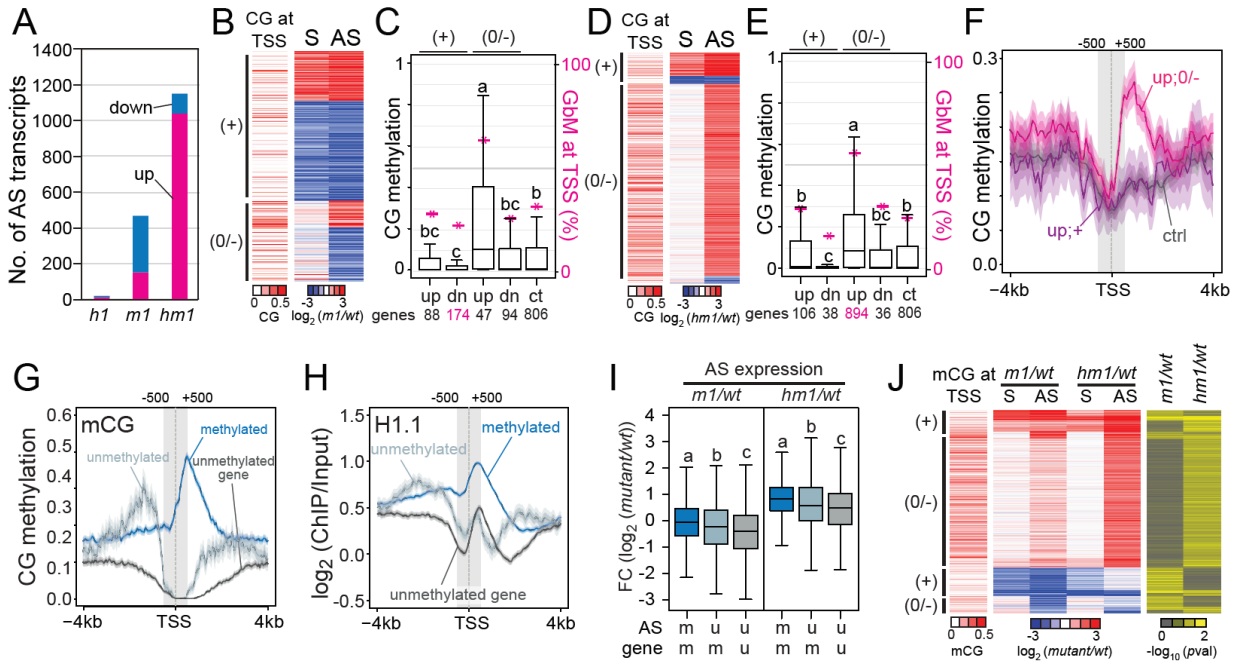

Figure 6. DNA methylation and H1 cooperatively suppress intragenic antisense transcripts. **(A)** Number of differentially expressed antisense (AS) transcripts in *h1, met1,* and *h1met1* plants. **(B and D)** Heat maps showing *wt* CG methylation at antisense TSS and expression of sense (S) and antisense transcripts in *met1* (B) or *h1met1* (D) plants. **(C and E)** Box plots of TSS-proximal *wt* CG methylation levels of upregulated (up) and downregulated (dn) antisense transcripts either positively correlated (+) or negatively/un-correlated (0/-) with sense expression in *met1* (C) or *h1met1* (E) plants. Data are also shown for unchanged (control; ct) antisense transcripts. Magenta asterisks indicate the percentage of antisense TSS that overlap gbM. "a", "b" and "c" are significantly different; overlapping letters – i.e. "b" and "bc" – indicate that the difference is not significant ($p < 0.01$; ANOVA). **(F)** *Wt* CG methylation around antisense TSS of indicated groups from (E) with more than 100 transcripts. Shaded areas represent 95% confidence intervals. **(G-H)** CG methylation (G) and H1.1 distribution (H) around the TSS of antisense transcripts initiated from unmethylated genes, unmethylated regions within gbM genes, and methylated regions within gbM genes. **(I)** Box plots of antisense expression in indicated groups from (G) in *met1* and *h1met1* plants. "a", "b" and "c" are significantly different ($p < 0.01$; ANOVA). **(J)** Heat maps of *wt* CG methylation at antisense TSS, expression of sense and antisense transcripts compared to *wt*, and corresponding antisense expression *p*-values in *met1* and *h1met1* plants. **(C, E and I)** Whiskers indicate 1.5X IQR.